VIP Molecular Imaging

DOI: 10.1002/anie.200800809

Detection of Enzymatic Activity by PARACEST MRI: A General Approach to Target a Large Variety of Enzymes**

Thomas Chauvin, Philippe Durand, Michèle Bernier, Hervé Meudal, Bich-Thuy Doan, Fanny Noury, Bernard Badet, Jean-Claude Beloeil, and Éva Tóth**

The search for physiologically responsive diagnostic probes is an important driving force in the current development of contrast agents for magnetic resonance imaging (MRI). Paramagnetic chemical exchange saturation transfer (PARACEST) agents hold promise as sensors for measuring various parameters of their biological environment (pH, temperature, metabolite or metal ion concentration).[1–5] PARACEST probes are ideally suited for molecular imaging since, as opposed to Gd^{3+}-based MRI agents, the contrast can be switched on and off at will.[6,7] They contain paramagnetically shifted mobile protons in slow exchange with bulk water. The irradiation of these protons affects the magnetic resonance signal of water protons through the chemical exchange. Factors influencing the exchange will have a detectable effect on the water signal. One drawback of PARACEST imaging is its modest sensitivity; typically millimolar concentrations of the agent are required,[8] and PARACEST detection of target molecules is not possible at low concentration. Enzymatic activation of a pro-PARACEST agent can circumvent this problem, as the transformation of a large amount of the agent can be realized through multiple enzyme-catalyzed cycles. Hence, PARACEST detection of enzyme activity can be possible even at low enzyme concentrations. In this perspective, Yoo et al. have recently developed a PARACEST probe that detects caspase-3.[9,10]

Here we report the first representative of a new, versatile platform of PARACEST agents designed for specific detection of a wide variety of enzymes. The molecular design is based on coupling an enzyme-specific substrate to a lanthanide-chelating unit through a self-immolative spacer (Scheme 1). After enzymatic cleavage of the substrate, the spacer is spontaneously eliminated which results in a concomitant change in the PARACEST properties of the Ln^{3+} chelate. In contrast to the previous enzyme-responsive agents,[9] this platform has the promise of being general and opening the way to specifically target a large variety of enzyme activities. While the Ln^{3+}-chelating unit and the self-immolative spacer can be identical for the entire family, the appropriate choice of the substrate will ensure enzyme specificity.

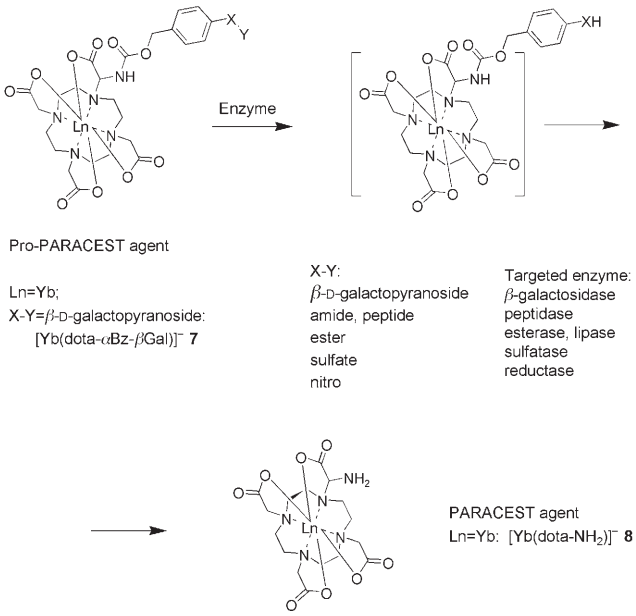

Scheme 1. Self-immolative degradation of the enzyme-specific agents. Bz = benzyl, dota = 1,4,7,10-tetraazadodecane-*N*,*N*′,*N*″,*N*‴-tetraacetate.

Self-immolative units are applied in antibody- or gene-directed enzyme prodrug therapy.[11–14] Some are based on the intrinsic instability of benzyloxycarbamates having an electron-donating substituent in the *ortho* or *para* position. With a benzyloxycarbamate as a self-immolative unit, the substrate can be any enzyme-recognized moiety capable of transitionally reducing the electron-donating capabilities of the phenyl substituent. In the context of MRI, Meade et al. have reported a Gd^{3+} complex with a self-immolative linkage, designed for detection of β-glucuronidase.[15]

In our approach, the self-immolative unit bearing the specifier is linked to one of the acetate arms of a Ln–dota unit through an α-carbamoyl nitrogen. Following the enzymatic attack and the resulting electron cascade. The electron cascade is not self-immolative, the carbamate is cleaved and transformed to an amine. The difference in the exchange rates and chemical shifts of the carbamate and the amine protons

[*] Dr. P. Durand, M. Bernier, Dr. B. Badet
Institut de Chimie des Substances Naturelles, CNRS
Avenue de la terrasse, 91198 Gif/Yvette Cedex (France)
Fax: (+33) 1-6907-7247
E-mail: philippe.durand@icsn.cnrs-gif.fr
T. Chauvin, H. Meudal, Dr. B.-T. Doan, F. Noury, Prof. J.-C. Beloeil, Dr. É. Tóth
Centre de Biophysique Moléculaire, CNRS
Rue Charles Sadron, 45071 Orléans Cedex2 (France)
Fax: (+33) 2-3863-1517
E-mail: eva.jakabtoth@cnrs-orleans.fr
Homepage: http://cbm.cnrs-orleans.fr/projets/p_organi.html

[**] This work was financially supported by the Centre National de la Recherche Scientifique, the Interdisciplinary program "Imagerie du Petit Animal" (CNRS), and European network (EMIL) no. 50356. It was performed within the European COST Action D38.

Supporting information for this article is available on the WWW under http://www.angewandte.org or from the author.

leads to a change in the PARACEST effect. To demonstrate this, we have synthesized [Yb(dota-αBz-βGal)]$^-$ **7**, which was designed to respond to the activity of β-galactosidase, a commonly used indicator of gene expression (Scheme 2; details in the Supporting Information).

PARACEST spectra were recorded before and after enzymatic reaction by applying selective saturation in 1 ppm increments from −90 to +90 ppm (data shown only between −50 and 30 ppm in Figure 1). No PARACEST effect is detectable for [Yb(dota-αBz-βGal)]$^-$ **7** although it contains a carbamate proton. It is surprising, since amide protons of Ln^{3+} complexes have been largely exploited in magnetization-transfer experiments. For carbamates, however, no proton-exchange data are available to our knowledge. After addition of *β*-galactosidase to a solution of **7** and incubation of the mixture (typically 31 U enzyme per 0.5 mL aliquot of 20 mM **7**, 37 °C, pH 7.5, 2 h),[16] PARACEST is observed at −16.7 and −20.5 ppm. The enzymatic reaction on [Yb(dota-αBz-βGal)]$^-$ **7** results in the self-immolative destruction of the spacer and yields [Yb(dota-NH_2)]$^-$ **8** (Scheme 1), as proved by LC-MS analysis of the reaction mixture following enzymatic cleavage. Hence we assigned the observed PARACEST effect to the two slowly exchanging, magnetically nonequivalent amine protons. Indeed, after enzymatic cleavage, two new signals appeared at −16.7 and −20.5 ppm in the ^{1}H NMR spectrum of the reaction mixture, while the peak at around −16 ppm, which we attributed to the carbamate proton of **7**, disappeared (see Figure S3 in the Supporting Information). It is worth mentioning that under certain conditions, typically at high enzyme and substrate concentrations, the reactive quinone methide that is formed during the degradation of the spacer can react with [Yb(dota-NH_2)]$^-$ **8** instead of water. This side reaction is practically abolished in the presence of carrier proteins like bovine serum albumin, as observed for the Gd analogue (see the Supporting Information). In addition, the enzymatic cleavage becomes faster when serum albumin is present. [Yb(dota-NH_2)]$^-$ **8** was also synthesized independently, and a PARACEST effect similar

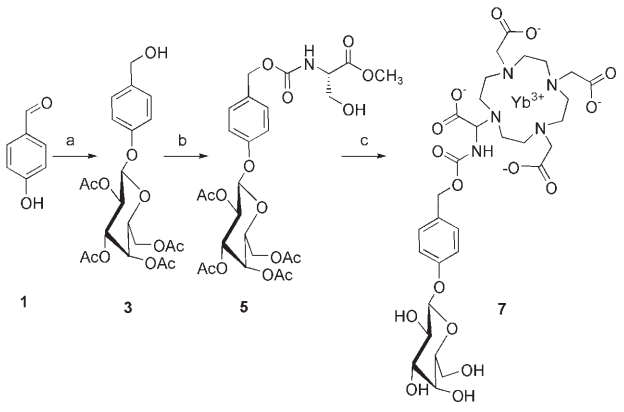

Scheme 2. Synthesis of [Yb(dota-αBz-βGal)]$^-$ **7**. a) 1. α-D-galactopyranosyl bromide, Ag_2O, CH_3CN (60%), 2. $NaBH_4$, *i*PrOH/CH_3Cl (78%); b) 1. *p*NO_2PhOCOCl, Pyr, EtOAc (93%), 2. methyl L-serine, Et_3N (84%); c) 1. $Pb(OAc)_4$, EtOAc (90%), b) Et_3DO_3A, TBD resin, c) NaOH pH 12, EtOH/H_2O, d) $YbCl_3$, pH 6.5 (22% overall yield). Et_3DO_3A = 1,4,7-tris(ethoxycarbonylmethyl)-1,4,7,10-tetrazacyclododecane, Pyr = pyridine.

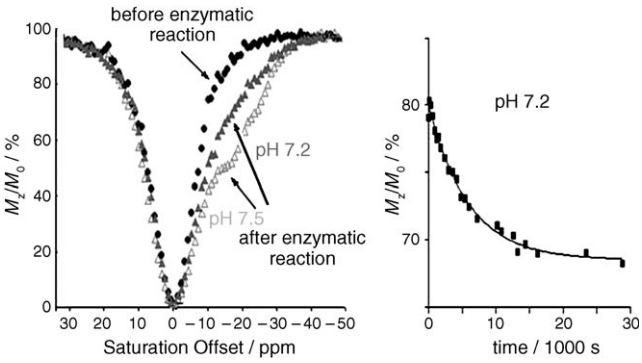

Figure 1. a) PARACEST spectra of [Yb(dota-αBz-βGal)]$^-$ **7** before and after reaction with *β*-galactosidase (pH 7.5 or 7.2). The spectra were acquired on a Bruker Avance 500 MHz NMR spectrometer with a continuous-wave saturation pulse of 31 μT for 3 s. c_{YbL} = 20 mM, 37 °C. b) Kinetics of enzyme-catalyzed hydrolysis of **7** monitored by means of the intensity of the water signal, with selective saturation at −16.7 ppm.

to that observed after enzymatic cleavage of [Yb(dota-αBz-βGal)]$^-$ **7** was also detected (see the Supporting Information).

As amino protons usually undergo fast exchange, observation of a PARACEST effect is not expected. The slow proton exchange on [Yb(dota-NH_2)]$^-$ **8** is likely related to the remarkably low protonation constant of the noncoordinating exocyclic NH_2 group. Indeed, $\log K_H = 5.12 \pm 0.01$ was determined by pH potentiometry on the Gd^{3+} analogue of **8**, [Gd(dota-NH_2)]$^-$ ($K_H = [HL]/[L^-][H^+]$). The decrease of $\log K_H$ by roughly four orders of magnitude relative to typical values for amines is a consequence of the metal coordination of the neighboring carboxylate oxygen and endocyclic nitrogen atoms. Although $\log K_H$ can slightly differ for the Gd^{3+} and Yb^{3+} complexes, the amine in [Yb(dota-NH_2)]$^-$ **8** is very likely not protonated at the pH of the PARACEST experiments (pH > 7). Thus, the contribution of the protonated species to the proton exchange will be limited for **8**. A much slower exchange by means of direct proton abstraction from the NH_2 group is expected to be eventually effective; it is also observed for the exocyclic amino hydrogens of neutral adenosine.[17,18]

The pH affects saturation transfer by means of the pH dependence of the proton exchange. The observed PARACEST effect is the greatest at about pH 7.4, with a sharp decrease with decreasing pH and a smaller decrease in the basic region. We note that the pH effect is not identical on the two amine protons, as it was previously reported for the two NH_2 protons of an Yb^{3+} dota-tetraamide complex (see Figure S5 in the Supporting Information).[7]

The PARACEST effect also makes it possible to monitor the kinetics of the enzymatic cleavage. As an example, we measured the time-dependency of the M_z/M_0 values in a 20 mM solution of [Yb(dota-αBz-βGal)]$^-$ **7** (0.5 mL) after addition of 31 U of β-galactosidase. An exponential fit of the normalized M_z/M_0 values as a function of the incubation time resulted in the rate constant $k_{obs} = 1.7 \times 10^{-4}\ s^{-1}$ ($t_{1/2}$ = 68 min; Figure 1). This corresponds to a rate of $4 \times 10^{-5}\ \mu mol\, s^{-1}\, U^{-1}$, which is slightly higher than the rate previously reported for a similar self-immolative βGal system ($7.4 \times 10^{-6}\ \mu mol\, s^{-1}\, U^{-1}$).[19] Recently, enzymatically activated pro-

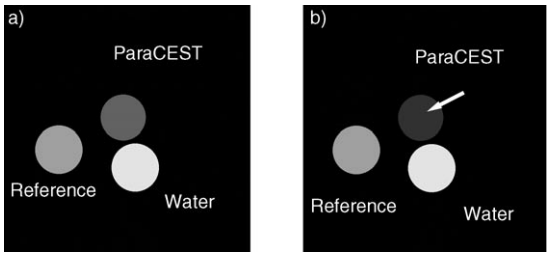

Figure 2. 400 MHz spin echo images of a phantom containing three tubes filled with water or a solution of 20 mM **7**$^{-}$ before and after enzymatic reaction; pH 7.5. a) Image with an irradiating continuous-wave pulse (3 s 25 μT) centered off resonance (16 ppm). b) Image recorded with an irradiating pulse centered on resonance (−16 ppm). The arrow shows the PARACEST effect.

drugs of doxorubicin containing a self-immolative benzyloxycarbamate linker with a galactose moiety have been also reported to have a slower hydrolysis ($t_{1/2}=217$ min).[20] For the cleavage of EgadMe, Meade et al. reported a V_{max} of 2.4×10^{-6} μmol s^{-1} U^{-1}.[21]

To further demonstrate the utility of the complex, we acquired MR images of a solution of 20 mM [Yb(dota-αBz-βGal)]$^{-}$ **7** before and after reaction with β-galactosidase, by applying a selective saturation at +16 ppm (off resonance) or −16 ppm (on resonance; Figure 2). The intensity of the signal is clearly weaker after enzymatic reaction. By subtracting the MR images with saturation offset of −16 ppm from the MR images with saturation offset of +16 ppm, we calculate a 29% ($[M_{off}-M_{on}]/M_{off}$) decrease in the water MR signal for the sample containing the enzymatically cleaved complex, while no significant change is obtained for the tubes with the noncleaved agent (1.8%) or with water (0.7%).

In conclusion, we have synthesized a first representative of a new family of molecular imaging agents that could offer the possibility of specific PARACEST detection for a large variety of enzymatic activities. This platform has several positive features: the substrate is at the extremity of a spacer that facilitates the enzymatic cleavage, and the PARACEST properties are not affected by the variation of the substrate. Since the PARACEST effect is observed after enzymatic activation, it can be optimized once for the whole family. The same Ln^{III} chelate and spacer will be applied for the detection of diverse enzymes by varying the substrate. The system works as a switch off/on probe, which can be a further advantage in practical in vivo or in vitro applications. Finally, these molecules are also prospective probes for the high- or medium-throughput screening of enzyme inhibitors by MRI. Most of currently used screening protocols are based on radiometric or spectrophotometric detection. Radiometric methods are hampered by the high cost and safety problems, while the spectrophotometric methods face the problem of numerous interferences which can lead to false positive or negative results. As MRI is much less prone to interferences, it might represent a viable alternative in high-throughput screening, provided that appropriate probes are available. Moreover, since β-galactosidase is a commonly used marker enzyme, this PARACEST system can also find application in the area of studying gene expression.[22]

Experimental Section

MRI saturation transfer experiments were performed at 400 MHz, 294 K on a Bruker Biospec 94/20 USR horizontal spectrometer equipped with 950 mT m^{-1} gradients, using a Bruker 35 mm shielded linear birdcage RF probe and running Paravision 4 software. Two multi-spin-echo RARE images (TR/TE 6 s/14 ms, na = 1, RARE factor = 8, FOV = 3 cm, resolution matrix 256 × 256, slice thickness 1 mm, duration 3 min) with the two offsets (−16 and + 16 ppm) of the irradiation MT pulse were recorded. The irradiation pulse was rectangularly shaped with a duration of 3 s and power of 25 μT.

Received: February 19, 2008
Published online: May 2, 2008

Keywords: imaging agents · lanthanides · PARACEST · proton exchange · saturation transfer

[1] S. Aime, D. D. Castelli, E. Terreno, *Angew. Chem.* **2002**, *114*, 4510; *Angew. Chem. Int. Ed.* **2002**, *41*, 4334.
[2] S. Zhang, R. Trokowski, A. D. Sherry, *J. Am. Chem. Soc.* **2003**, *125*, 15288.
[3] S. Zhang, M. Merritt, D. E. Woessner, R. E. Lenkinski, A. D. Sherry, *Acc. Chem. Res.* **2003**, *36*, 783.
[4] J. A. Pikkemaat, R. T. Wegh, R. Lamerichs, R. A. van de Molengraaf, S. Langereis, D. Burdinksi, A. Y. F. Raymond, H. M. Janssen, B. F. M. de Waal, N. P. Willard, E. W. Meijer, H. Grüll, *Contrast Media Mol. Imaging* **2007**, *2*, 229.
[5] R. Trokowski, J. Ren, F. K. Kalman, A. D. Sherry, *Angew. Chem.* **2005**, *117*, 7080; *Angew. Chem. Int. Ed.* **2005**, *44*, 6920.
[6] S. Zhang, P. Winter, K. Wu, A. D. Sherry, *J. Am. Chem. Soc.* **2001**, *123*, 1517.
[7] S. Zhang, L. Michaudet, S. Burgess, A. D. Sherry, *Angew. Chem.* **2002**, *114*, 1999; *Angew. Chem. Int. Ed.* **2002**, *41*, 1919.
[8] S. Aime, S. G. Crich, E. Gianolio, G. B. Giovenzana, L. Tei, E. Terreno, *Coord. Chem. Rev.* **2006**, *250*, 1562.
[9] B. Yoo, M. D. Pagel, *J. Am. Chem. Soc.* **2006**, *128*, 14032.
[10] B. Yoo, M. S. Raam, R. M. Rosenblum, M. D. Pagel, *Contrast Media Mol. Imaging* **2007**, *2*, 189.
[11] P. L. Carl, P. K. Chakravarty, J. A. Katzenellenbogen, *J. Med. Chem.* **1981**, *24*, 479.
[12] J.-L. Guerquin-Kern, A. Olk, E. Chenu, R. Lougerstay-Madec, C. Monneret, J.-C. Florent, D. le Carrez, A. Croisy, *NMR Biomed.* **2000**, *13*, 306.
[13] R. Madec-Lougerstay, J.-C. Florent, C. Monneret, *J. Chem. Soc. Perkin Trans. 1* **1999**, 1369.
[14] F. M. H. deGroot, W. J. Loos, R. Koekkoek, L. W. A. van Berkom, G. F. Busscher, A. E. Seelen, C. Albrecht, P. de Bruijn, H. W. Scheeren, *J. Org. Chem.* **2001**, *66*, 8815.
[15] J. A. Duimstra, F. J. Femia, T. J. Meade, *J. Am. Chem. Soc.* **2005**, *127*, 12847.
[16] 1 U of the enzyme is able to hydrolyze 1 μmol of *p*-nitrophenyl-β-D-galactoside per minute.
[17] B. McConnell, *Biochemistry* **1974**, *13*, 4516.
[18] D. G. Cross, A. Brown, H. F. Fisher, *Biochemistry* **1975**, *14*, 2745.
[19] A. K. Ghosh, S. Khan, D. Farquhar, *Chem. Commun.* **1999**, 2527.
[20] H. Devalapally, R. S. Navath, V. Yenamandra, R. R. Akkinepally, R. K. Devarakonda, *Arch. Pharmacal Res.* **2007**, *30*, 723.
[21] A. Y. Louie, M. M. Hüber, E. T. Ahresn, U. Rothbächer R. Moats, R. E. Jacobs, S. E. Fraser, T. J. Meade, *Nat. Biotechnol.* **2000**, *18*, 321.
[22] N. H. Ho, R. Weissleder, C.-H. Tung, *ChemBioChem* **2007**, *8*, 560.

